AFRL-RD-PS-
TP-2023-0009

# GEOSYNCHRONOUS SATELLITE DETECTION AND TRACKING WITH WFOV CAMERA ARRAYS USING SPATIO-TEMPORAL NEURAL NETWORKS (GEO-SPANN)

**Garrett Fitzgerald**

**22 February 2022**

**Technical Paper**



**AIR FORCE RESEARCH LABORATORY**
**Directed Energy Directorate**
**3550 Aberdeen Ave SE**
**AIR FORCE MATERIEL COMMAND**
**KIRTLAND AIR FORCE BASE, NM 87117-5776**

# REPORT DOCUMENTATION PAGE

| 1. REPORT DATE | 2. REPORT TYPE | 3. DATES COVERED | |
|---|---|---|---|
| 22 February 2022 | Paper | START DATE | END DATE |

**4. TITLE AND SUBTITLE**

GEOSYNCHRONOUS SATELLITE DETECTION AND TRACKING WITH WFOV CAMERA ARRAYS USING SPATIO-TEMPORAL NEURAL NETWORKS (GEO-SPANN)

| 5a. CONTRACT NUMBER | 5b. GRANT NUMBER | 5c. PROGRAM ELEMENT NUMBER |
|---|---|---|
| | | |
| **5d. PROJECT NUMBER** | **5e. TASK NUMBER** | **5f. WORK UNIT NUMBER** |
| | | No associated work unit number |


**6. AUTHOR(S)**

Garrett Fitzgerald

**7. PERFORMING ORGANIZATION NAME(S) AND ADDRESS(ES)**

Air Force Research Laboratory
550 Lipoa Parkway
Kihei, HI 96753


**8. PERFORMING ORGANIZATION REPORT NUMBER**

| 9. SPONSORING/MONITORING AGENCY NAME(S) AND ADDRESS(ES) | 10. SPONSOR/MONITOR'S ACRONYM(S) | 11. SPONSOR/MONITOR'S REPORT NUMBER(S) |
|---|---|---|
| | AFRL/RDSM | AFRL-RD-PS-TP-2023-0009 |

**12. DISTRIBUTION/AVAILABILITY STATEMENT**

Distribution A:
Approved for public release; distribution is unlimited. Public Affairs release approval # AFRL-2022-1095

**13. SUPPLEMENTARY NOTES**


**14. ABSTRACT**

Detection of low resolution, deep-space objects in wide field of view (WFOV) imaging systems can benefit from the emergence of temporally learned, appearance based detectors. The PANDORA sensor array, located in Maui at the Air Force Maui Optical and Supercomputing Site, is an exemplar of a scalable imaging architecture which can detect dim deep space objects while maintaining a WFOV. The PANDORA system captures 20x120 degree images of the night sky oriented along the GEO belt at a rate of two frames per minute. Prior work has established a baseline performance for the detection of Geosynchronous Earth Orbit (GEO) satellite objects using classical, feature based detectors, but has not leveraged the temporally rich data captured by PANDORA.This work extends the GEO object detection and tracking problem by implementing a spatio-temporal deep learning architecture (GEO-SPANN), further improving the state of the art in low resolution, deep-space object detection. Annotated sequential frames including object motion are used to train GEO-SPANN, which uses a two-stage CNN to provide a learned temporal mapping of GEO objects in sequences of annotated PANDORA images. We present the GEO object detection and tracking results of GEO-SPANN on sequences of 100 frames of PANDORA data. GEO-SPANN advances strategies for autonomous detection and tracking of GEO satellites, allowing PANDORA to be leveraged for orbit catalogue maintenance and space object anomaly detection.



**15. SUBJECT TERMS**

Space Situational Awareness, WFOV, object detection, spatio-temporal neural networks


| 16. SECURITY CLASSIFICATION OF: | | | 17. LIMITATION OF ABSTRACT | 18. NUMBER OF PAGES |
|---|---|---|---|---|
| a. REPORT | b. ABSTRACT | C. THIS PAGE | | |
| Unclassified | Unclassified | Unclassified | SAR | 12 |

| 19a. NAME OF RESPONSIBLE PERSON | 19b. PHONE NUMBER *(Include area code)* |
|---|---|
| Garrett Fitzgerald | |



PREVIOUS EDITION IS OBSOLETE.

**STANDARD FORM 298 (REV. 5/2020)**
*Prescribed by ANSI Std. Z39.18*

# Geosynchronous satellite detection and tracking with WFOV camera arrays using spatio-temporal neural networks (GEO-SPANN)

Garrett Fitzgerald[a], Ruixu Liu[a], and Vijayan Asari[a]

[a]University of Dayton, Department of Electrical and Computer Engineering, Dayton, OH, USA

## ABSTRACT

Detection of low resolution, deep-space objects in wide field of view (WFOV) imaging systems can benefit from the emergence of temporally learned, appearance based detectors. The PANDORA sensor array, located in Maui at the Air Force Maui Optical and Supercomputing Site, is an exemplar of a scalable imaging architecture which can detect dim deep-space objects while maintaining a WFOV. The PANDORA system captures 20x120 degree images of the night sky oriented along the GEO belt at a rate of two frames per minute. Prior work has established a baseline performance for the detection of Geosynchronous Earth Orbit (GEO) satellite objects using classical, feature based detectors, but has not leveraged the temporally rich data captured by PANDORA. This work extends the GEO object detection and tracking problem by implementing a spatio-temporal deep learning architecture (GEO-SPANN), further improving the state of the art in low resolution, deep-space object detection. Annotated sequential frames including object motion are used to train GEO-SPANN, which uses a two-stage CNN to provide a learned temporal mapping of GEO objects in sequences of annotated PANDORA images. We present the GEO object detection and tracking results of GEO-SPANN on sequences of 100 frames of PANDORA data. GEO-SPANN advances strategies for autonomous detection and tracking of GEO satellites, allowing PANDORA to be leveraged for orbit catalogue maintenance and space object anomaly detection.

**Keywords:** Space Situational Awareness, WFOV, object detection, spatio-temporal neural networks

## 1. INTRODUCTION

### 1.1 WFOV Sensors for SDA

For defense and commercial space operations, Space Domain Awareness (SDA) is contingent on the tasking bandwidth of ground-based electro-optical (EO) telescope systems. The capacity of EO systems to discover, track, and characterize resident space objects (RSOs) allows for the effective employment and operation of satellites in all orbits. Narrow field-of-view optical (NFOV) EO systems- often, large aperture optical telescopes- are the most prominent instruments used in the monitoring of RSOs. With the proliferation of near-Earth RSOs, the demand for ground-based observations grows in proportion, putting stress on NFOV EO system tasking. In order to effectively allocate the finite resources of NFOV EO systems, wide field-of-view (WFOV) optical systems present a means to augment SDA resources by providing observations of multiple RSOs over larger regions of the sky. With WFOV EO systems, NFOV telescope tasking can be informed to high priority targets, including anomalous satellite behavior such as combatant maneuvering and collision warning. In tandem, the pairing of WFOV and NFOV sensor systems can more effectively provide RSO catalog maintenance, with the output of WFOV systems used to cue NFOV systems.[1]

This proposed division of labor between high-fidelity, low-obsevation-bandwidth NFOV systems and low-sensitivity, high-observation-volume WFOV systems motivates the development of WFOV EO systems. One design solution which is cost-effective and scalable uses commercial off the shelf (COTS) camera arrays which passively acquire imagery of the sky. The data from redundant camera arrays can be used to monitor the concurrent activity of hundreds of satellites with reasonable sensitivity. With a matured WFOV EO system, a large fraction of the RSO population can be tracked from a single sensor system, freeing up collection capacity for high-resolution NFOV EO systems while also providing tasking information.

### 1.2 PANDORA WFOV Camera Array

The PANDORA (Persistent AND Optically Redundant Array) 9x5 COTS camera array, developed by Tau Technologies, is a WFOV sensor solution to fill the role of a high-observation-volume EO system. Oriented to passively capture imagery along the GEO belt, PANDORA utilizes 9 neighboring fields of redundant imagery to acquire a 120x20deg view of the sky. Each of the 9 fields in the sensor array covers a 15x20 view of the sky, and is composed of 5 cameras in common-field. The imagery of these same-field cameras is combined to improve SNR and allow for dim-object light detection. Completed stacked imagery for each field is processed at a rate of 1/30 Hz with an effective exposure time of 60 seconds per frame, accomplished by alternating and co-adding exposures between common-field cameras. With overlap between the 9 fields, the total field of view of the system is 120x20 deg, providing the ability to persistently and passively monitor RSOs.

After post-processing, the PANDORA camera array yields 9 (5776x4224x16b) images twice per minute. With over 220 megapixels in the 9 stacked frames, the detection of GEO RSOs is an incredibly low-resolution problem, with each GEO object sized around 3x3 pixels. Light from RSOs of Medium Earth Orbit (MEO) and Low Earth Orbit (LEO), along with other orbital regimes, are also collected by the system, and are also low in pixel resolution. The feature space of the imagery is dominated by the long-exposure light smears of stars, with crowded fields containing the light of millions of stars. The detection of RSOs in all-sky single frames of imagery is a difficult task for a human observer, which makes annotation of PANDORA imagery very time consuming and expensive. Furthermore, the data volume and velocity of the system is immense; over the course of an observing night, the system produces roughly 800 GB of stacked imagery. Combined, these characteristics make the development of computer vision and image processing methods for automated RSO monitoring very challenging.

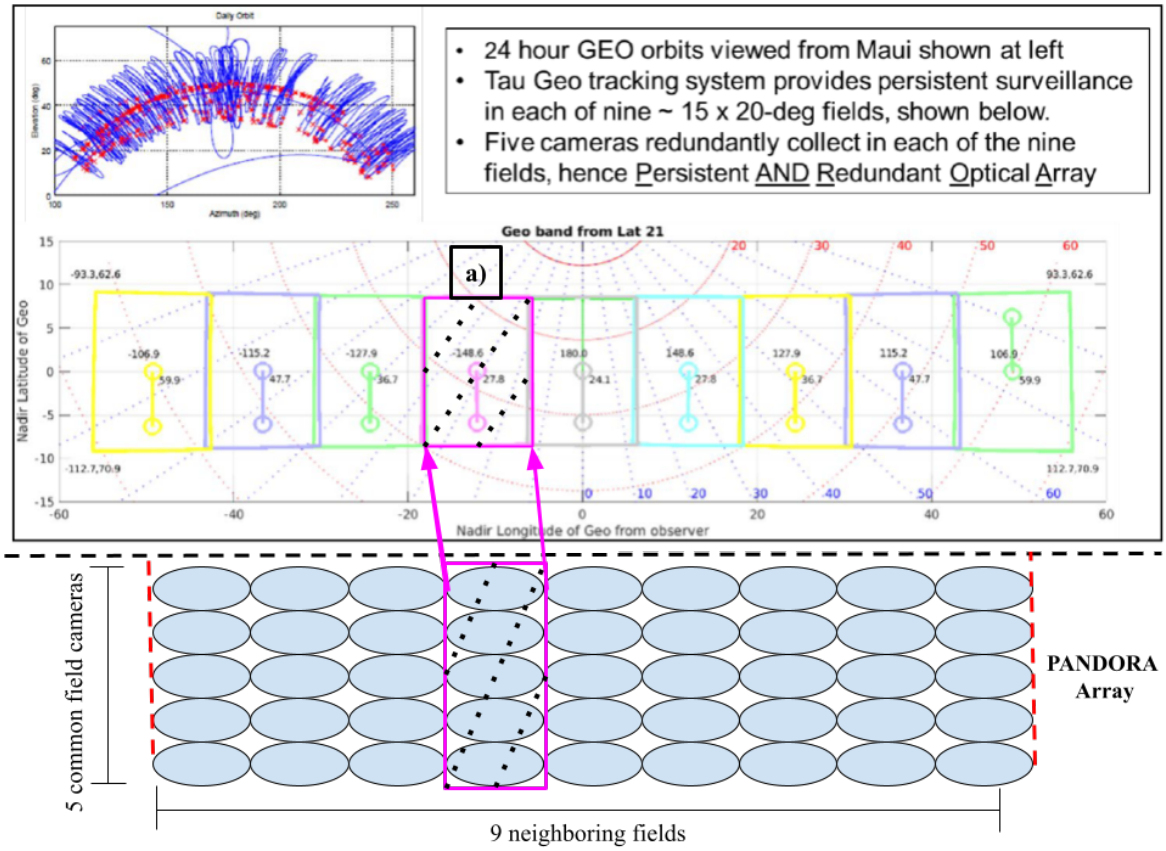


Figure 1: PANDORA array geometry relative to total 20×120 FOV, with a single 20°×15° field, **a)** highlighted with its corresponding 5 overlapping sensors.

### 1.3 Object Detection in PANDORA

Automated object detection is a necessary technology to fully deploy the PANDORA sensor, as the manpower and time required to manually monitor RSOs is not feasible. Deep learning techniques for object detection have proven to be reliable in all fields involving computational imagery, but there is limited literature on object detection for such low resolution targets in WFOV imagery. Recent work in Wide Area Motion Imagery (WAMI) has demonstrated the effectiveness of spatio-temporal neural networks for object detection in a similar feature space, and is used as inspiration for this work.

PANDORA provides nightly deep-space surveillance at the Air Force Maui Optical and Space Surveillance Site (AMOS), which motivates the development of an image processing pipeline to exploit its data. Prior work established a baseline for single frame GEO RSO detection using classical, feature based detection techniques.[2] This previous work used synthetic PANDORA data, which was a surrogate necessitated by the lack of annotated physical PANDORA data. With the completion of an annotated PANORA dataset, this work is the first to use deep learning techniques on a comprehensive annotated physical WFOV dataset. The architecture developed in this paper, GEO-SPANN, implements a spatio-temporal neural network to detect RSOs in PANDORA imagery, improving on the previous results using classical object detection methods.

An overview of related works is detailed in Section 2, including a review of similar sensor concepts and applicable WAMI efforts. Section 3 describes the dataset used in this paper, including the annotation methodologies and sensor attributes. Section 4 details the image processing pipeline developed, including a detailed description of GEO-SPANN. Section 5 details experiments executed to quantify object detection and tracking performance. Section 6 summarizes results and contributions of this paper along with plans for future work.

## 2. RELATED WORKS

While an important and emerging sensing concept, there is limited literature available on WFOV sensor technologies used in the realm of SDA. Notable work which motivates the use of WFOV sensors is detailed. Similar sensors to PANDORA have been developed, but there is sparse literature on exploiting this data for the purpose of monitoring GEO RSOs. Other work which exploits ground-based EO for RSO monitoring can be used, and much progress has been made in creating deep learning techniques to accurately detect RSOs in NFOV telescopes. A similar field in computer vision, WAMI, can be leveraged to aid in the development of methods to detect and track low-resolution objects in WFOV data. WAMI has seen much improvement in recent years with the use of spatio-temporal neural networks for object detection and tracking; these efforts are detailed. As a relatively novel sensing concept, we must look for solutions using similarly WFOV and temporally rich data. Related work in the realm of SDA, astronomy, and wide area surveillance are used to inform the motivations and technological goals for this work.

### 2.1 WFOV Passive Sensing for SDA

WFOV camera array sensing concepts in the visible regime which achieve all-sky coverage have not been widely studied in the application of detecting and tracking GEO objects. Although orbit estimation models have been formulated for this problem,[3] the computer vision problem of exploiting all-sky data with object detection algorithms requires a novel approach, as explored in this paper. Outside of our previous work,[2] there are no published techniques available for detecting stationary or near-stationary GEO RSOs in WFOV data. We aim to improve on previous baseline work using deep learning, which has had much success in RSO detection.[4]

The notion of utilizing a collaborative system of shared SDA custody for satellite tracking between a passive, all-sky system and higher resolution telescopes has been explored in recent years, notably with the Raven-class telescope,[5] and with a PANDORA system for detection of low earth orbit (LEO) objects.[6] Other COTS camera arrays used for various SDA applications such as,[7] and,[8] have shown the effectiveness of using co-added sensor exposures of a common field of view to achieve an improved SNR of low light objects. PANDORA implements this COTS co-added sensing concept, with an improved SNR proportional to the number of overlapping sensors.[9] Like PANDORA, the sensor arrays in,[7] and[8] are cheap and scalable, utilizing COTS components. Unlike PANDORA, these WFOV systems are applied to such problems as star streak detection and general synoptic surveys, and have not been used for GEO object monitoring.

Similar to PANDORA, some recent optical astronomy initiatives have taken an indiscriminate approach to data collection, including synoptic surveys such as those in progress with the Vera Rubin Telescope, or LSST.[10] These approaches require comprehensive data management strategies,[11] and the development of computer vision algorithms to sift through large quantities of data. However, systems collecting optical data in this manner have not yet been used in the detection and tracking of GEO objects, or any relatively stationary space objects similar to GEO satellites. We aim to create methods to process PANDORA image data, allowing for the system to be employed in autonomous monitoring of GEO objects' orbit determinations, catalog maintenance, and anomaly detection.

### 2.2 Object Detection in WFOV EO Systems

Without computer vision methods available for any related sensors, the problem of detecting satellites in crowded and large fields requires shifting from the realm of SDA and WFOV astronomy into a well-known class of research, which can be leveraged in the development of PANDORA's image processing strategies. In order to exploit image data from the PANDORA system, we frame the object detection as a Wide Area Motion Imagery (WAMI) problem. WAMI literature is rich in algorithm development for object detection in WFOV imagery, and has demonstrated success in a wide range of applications. WAMI architecture performance on similar problems provides context for the PANDORA processing pipeline.[12–14]

WAMI object detection algorithms generally rely on something that is not applicable to PANDORA data: a static background. The standard process for WAMI detection pipelines involve frame differencing and background subtraction, resulting with candidate regions of object motion in which feature detection techniques are employed.[15] As PANDORA image background is not static, this approach is not acceptable for our use case. If GEO objects were completely stationary temporally, a reverse to this process could yield regions of the frame with no motion. However, this temporal scene feature is not applicable, as GEO objects are not completely stationary. WAMI algorithms of interest are those which can detect objects based on their local features,[16].[17] Detection algorithms in these papers are used as inspiration for the detection algorithms explored in this paper. With a breadth of WAMI object detection schemes as inspiration for the PANDORA processing pipeline, we adapt WAMI methodologies for satellite detection in WFOV imagery of PANDORA.

### 2.3 Spatio-temporal Neural Networks for WFOV Obejct Detection and Tracking

Computer vision object detection approaches utilizing neural networks have been proven to broadly outperform the best classical object detection algorithms, notably with work demonstrated in Faster R-CNN,[18] ResNet,[19] and YOLO 9000.[20] However, the detection problem in these papers use datasets with object candidates comprising most of the image frame,[21] while in PANDORA imagery, a given GEO object may be 3×3 pixels in a 220MP image. This large search space, combined with the relative size of objects compared to the scene size, render the direct adoption of proven CNNs for object detection unsuitable. Recent efforts in WAMI have extended the use of spatio-temporal neural networks to achieve state of the art in WAMI moving object detection.[22–25] These works assert that modifications to learned spatial detectors can yield state-of-the-art results for the WAMI task of tracking cars in WFOV data. We can directly adapt these architectures, especially that of,[22] as the feature space of PANDORA data is similar to the WAMI data used. GEO-SPANN uses a two-stage spatio-temporal similar to,[22] with modifications to account for varying classes of RSOs.

## 3. DATASETS

For the first time, human-annotated physical PANDORA data is available via pre-release for use in the training and testing of RSO detection and tracking algorithms. This pre-release data, designated SatNet-PANDORA-v0, contains over 10,000 images and corresponding annotations from the PANDORA sensor. Annotations contain a bounding box and center point for each object, along with the extents of the bounding box. Annotated objects include RSOs of different orbital regimes, including LEO, MEO, and GEO, but their distinct classification via orbital regime is not specified in annotation metadata. All SatNet-PANDORA-v0 images are 5776x4224x16b, and correspond to one of 9 fields of the PANDORA sensor. An example full field with associated annotations is shown in Figure 3. Examples of RSOs in the annotated dataset are shown in Figure 4. The observations used for this dataset were all taken on the night of April 20, 2021, and all 9 fields of the sensor have been annotated

for the course of the entire night. In total, there are 9 sets of roughly 1500 sequential images, representing an observing run of around 12 hours.

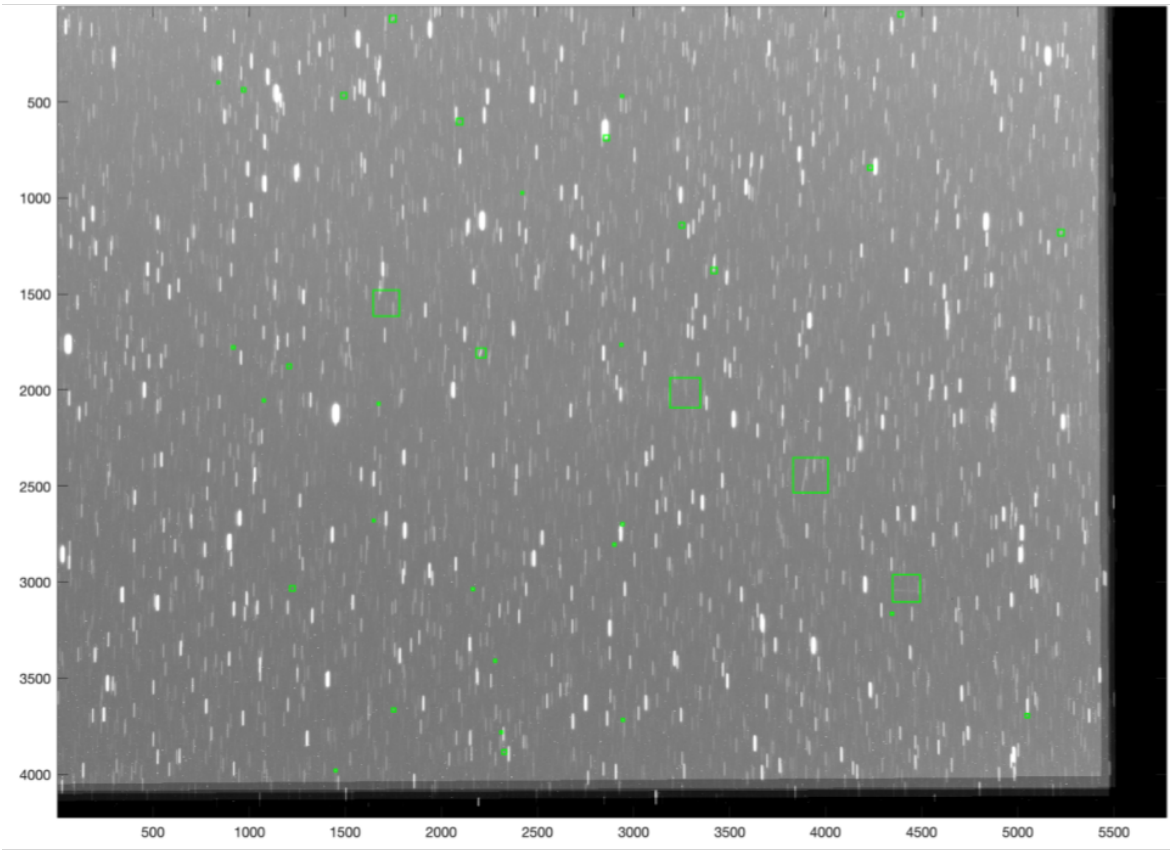


Figure 2: A full 20x15 deg field of PANDORA data shown with annotations in green. Note the extremely low resolution of the annotated objects, necessitating the rigorous, SILT-aided labeling process.

### 3.1 Annotation Methodology

The annotation of such large quantities of imagery each with vast search areas and low resolution objects of interest is a challenging and time consuming task requiring meticulous attention. Enabled Intelligence's annotation team uses trained analysts, assisted by annotation assistance software developed specifically for PANDORA data. This tool, developed by KBR, is called the Space Labeling Imaging Tool (SILT). SILT allows the analysts to break the large images up into smaller tiles and examine them temporally to find and label objects of interest. SILT can linearly interpolate object motion and label sequential frames, improving the annotation process. Annotations are square bounding boxes of various size, as the footprint of RSOs in different orbits vary considerably. Roughly 1000 frames can be annotated per week, and each batch is subject to QA review to ensure a high level of accuracy. Still, there may be some errors in labeling all objects which are detectable by the sensor (ie, a satellite whose reflected light is detected by the sensor, but whose SNR is so close to 1 that a human may not be able to distinguish from background). As with all human-annotation regimes, there are limitations to the established ground truth. This annotated dataset is made robust with the use of SILT, but there remains a bias to brighter objects.

### 3.2 System Noise and Data

There are multiple sources of noise in PANDORA imagery, including atmospheric turbulence, detector integration, dark current, and optics diffraction. Beyond the inherent noise in the computational imagery acquisition

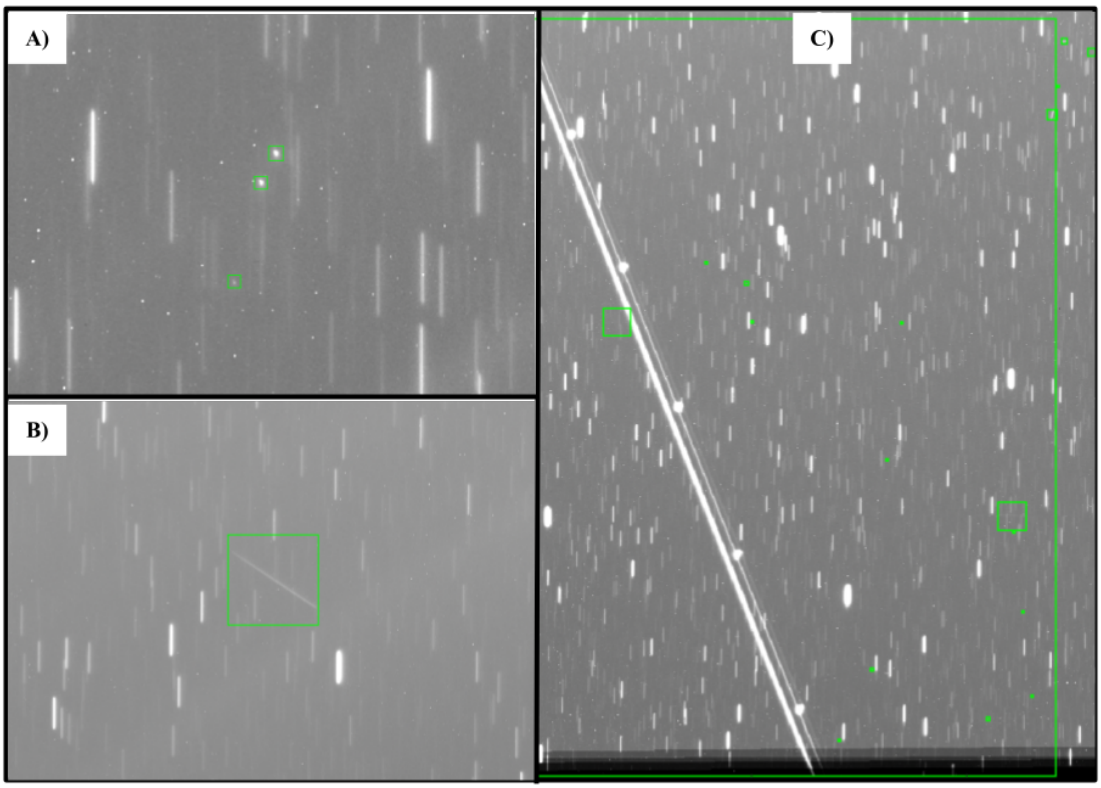


Figure 3: Various RSOs of different orbital regimes and resulting morphology. A cluster of GEO RSOs are annotated in (A), a low-light MEO RSO is highlighted in (B), and a bright streaking LEO RSO is shown in (C).

process, there are additional sources of error from the image stacking process. The effects of dark current (hot pixels) and detector integration noise (dead pixels) are compounded, as each processed image is the composite of multiple exposures from multiple cameras. The resulting impact of noise is noticeable in the form of heavy salt and pepper noise throughout the scene. This noise complicates the object detection problem, as GEO satellites are very similar in features to the bright pixel noise, as evidenced in Figure 5. Unfortunately, as the imagery available is already processed and the raw frames are not available, methods to restore a non-noisy scene are not possible. Bad pixel masks can be used to smooth the static noise, and this approach will be included in the experiments. Sensor inherent noise, while not too large a factor in high resolution object detection, plays a much larger role in WFOV object detection.

Data is partitioned in temporal sequences, as the overall goal of this work is to detect and track RSOs. As SatNet-PANDORA-v0 is made up of a single night of data, in order to create diverse conditions for object motion and RSO population, the 9 fields are broken up into hour-long chunks for training and testing. This strategy for data preparation is not ideal, especially considering the substantial variations in observing conditions from night to night. A more diverse set of observations would make for results of this work to be more representative of real world conditions. One possibility to augment the available annotated PANDORA data would be to use the SatSim-PANDORA synthetic dataset.[2] However, with more annotations scheduled for physical PANDORA data, the synthetic data should be mainly used to train and test on rare observation scenarios. Synthetic imagery can be used to augment the training data for scenarios which are not found in observations, such as satellite collision.

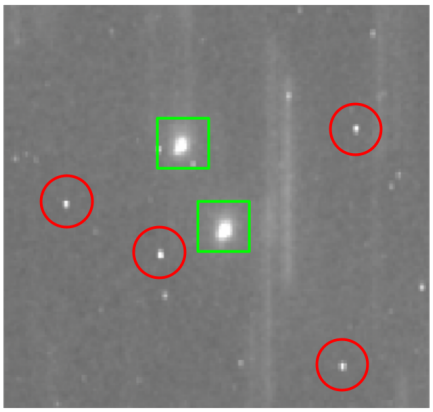

Figure 4: Zoom-in section including GEO RSOs (outlined by green squares) and bright pixel noise (outlined by red circles). The hot pixel noise is fixed; GEO RSOs are distinguished temporally, as they will often move slightly from frame to frame.

## 4. METHODS

The priorities for a learned solution to RSO detection in PANDORA data include efficiency (due to the WFOV imagery and search space), the leveraging of rich temporal features, and high precision. As discussed in Sec. 2.3, recent literature on WAMI object detection provides some examples of spatio-temporal neural networks which will serve as a basis for GEO-SPANN. Our solution follows a similar strategy to that proposed in.[22] GEO-SPANN is a two-stage spatio-temporal convolutional neural network (CNN), which first proposes a heatmap of regions of interest (ROI) to reduce the search space, and then feeds the heatmap of probable object locations to a object detector, which predicts the bounding box of the RSO. Later, we expand this design to operate as both a detector and re-identifier of previously detected objects, which will allow for the tracking of RSOs.

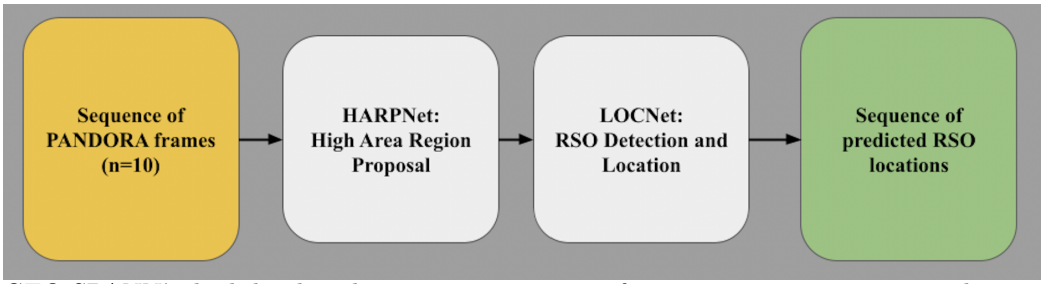


Figure 5: GEO-SPANN's high-level architecture, consisting of a two-stage spatio-temporal neural network. HARP-Net and LOC-Net are designed for the efficent detection of low-resolution, temporally shifting objects in PANDORA data.

### 4.1 HARP-Net: Region Proposal by Exploiting Motion

A learned reduction in the search space for our detector is accomplished in the first stage of GEO-SPANN, using a 2D CNN with stacked temporal frames to output their respective heatmaps of ROIs. This first stage, called HARP-Net (High Area Region Proposal), is created using a fully convolutional neural network. HARP-Net downsamples the large PANDORA imagery using convolutional strides and max pooling. Sequential frames are used as input to this 2D CNN to exploit the scene's temporal information. A central frame acts as a pivot to the $h$ previous and $w$ subsequent frames, and in this manner a set of N frames can be input. Each frame learns its own convolutional filter set, and then are combined around the pivot frame to produce feature maps. The 2D CNN comprising HARP-Net uses the following equation:

$$f_{x,y} = \sum_{n=1}^{N} \left[ \sum_{i=1}^{k_h} \sum_{j=1}^{k_w} V_n(i,j) K_n(k_h - i, k_w - j) \right] + b_m, \quad (1)$$

Where $V_n$ is the $n^{th}$ frame in the temporally connected stack, $K_n$ is the convolutional kernel for frame $n$ of size $(k_h, k_w)$ to compute feature map values $f^m \in \mathbb{R}^M$, where $M$ is the set of feature maps, $n \in$ is a frame in the set of temporal frames, and $b_m$ is a learned bias to feature map $m$. A heatmap-based formulation is the output for this stage, which indicates learned ROIs with the temporal context around the central frame. Notably, we can choose which central frame $n$ we will maximize via back propagation between the output heatmap and ground truth.

### 4.2 LOC-Net: Object Detection with Reduced Search Space

The second stage of GEO-SPANN will take the reduced search space output and use a spatial detector to bound the predicted objects in a sequence of frames. LOC-Net, which uses YOLOv5, works on the knowledge that via the previous step, each output pixel essentially gives a vote whether it is a pixel containing a potential RSO. Areas which contain a high output value are cropped from HARP-Net and used as input to LOC-Net. The spatial information in the scene is cropped to contain connected ROI pixels above a threshold value. Effectively, we can ignore large areas of the scene which do not have ROI pixels above threshold, and then train a YOLO detector to predict new bounding boxes for RSOs in the scene.

## 5. RESULTS

SatNet-PANDORA-v0 is broken into 100 sets of 100 sequential frames for experiments. We will use 90 sets of 100 frames for training of GEO-SPANN, and 10 sets for testing. Performance is measured in precision, recall, and max F1 score, where we determine a true positive to be within a pixel euclidean distance $\theta$ of an annotation. Furthermore, while the annotated dataset does not classify different classes of RSO, we also provide a prediction for 3 main classes: GEO, MEO, and LEO RSOs. GEO-SPANN was built using TensorFlow, and was GPU accelerated.

Table 1: GEO-SPANN Object Detection Performance on Each Test Data Set

| Dataset | $F_1^*$ | Precision at $F_1^*$ | Recall at $F_1^*$ | TP at $F_1^*$ | FP at $F_1^*$ | FN at $F_1^*$ |
|---|---|---|---|---|---|---|
| Test Set 1 (TS1) | 0.82 | 0.746 | 0.79 | 172 | 19 | 238 |
| TS2 | 0.866 | 0.68 | 0.75 | 75 | 212 | 225 |
| TS3 | 0.757 | 0.971 | 0.69 | 166 | 22 | 234 |
| TS4 | 0.770 | 0.78 | 0.66 | 155 | 22 | 155 |
| TS5 | 0.801 | 0.88 | 0.76 | 155 | 18 | 210 |
| TS6 | 0.891 | 0.96 | 0.83 | 169 | 13 | 210 |
| TS7 | 0.839 | 0.82 | 0.7 | 180 | 10 | 222 |
| TS8 | 0.752 | 0.8 | 0.71 | 151 | 13 | 221 |
| TS9 | **0.945** | 0.96 | 0.93 | 217 | 3 | 225 |
| TS10 | 0.861 | 0.76 | 0.89 | 209 | 23 | 234 |
| AVERAGE | 0.87 | 0.91 | 0.83 | 214 | 19 | 204 |

Table 1 shows the results of GEO-SPANN performed on the 10 sets of test data. There are 100 frames per set, and we report the average detection metrics for the whole series of frames. We see that there is an average $F_1^*$ of 0.87 for the entire test dataset, which is a very solid baseline for object detection. We extended the single frame detection performance to include temporal information contained in GEO-SPANN, and found that when we repeat the above experiments, we have an average increase in the average $F_1^*$, resulting with a score of 90.1. These are encouraging results for this methodology in detecting low resolution objects in WFOV data.

## 6. CONCLUSION AND FUTURE WORK

The spatio-temporal neural network (GEO-SPANN) approach implemented in this work improves object detection in PANDORA data while also creating an efficient means to produce RSO detection and tracking information. This computer vision technology is essential to the utilization of WFOV passive sensors. Techniques introduced will play a major role in the future of space surveillance as our orbital regimes are increasingly populated and the demand for a high-volume all-sky sensor is required. With GEO-SPANN, we have remarkably high precision in the detection of RSOs, with the added benefit of being able to discriminate between different classes of space objects. This network would benefit from a variety of observing conditions for training, but we can assert that it is now a benchmark for state of the art in this class of WFOV RSO detection. Future work will use the detection methods introduced here and extend them to produce tracks of space objects, which can be used in a hierarchical structure of WFOV and NFOV sensors.

## ACKNOWLEDGMENTS

The author would like to thank Ian Mcquaid, Justin Fletcher, Capt Zachary Funke and the teams at AFRL/Maui and KBR/Centauri for enabling access to data and the support in this graduate degree effort. There would be no way to produce a deep learning solution to this problem without the annotators at Enabled Intelligence, whose diligence allowed for this work. Also, thanks to the ECE dept at the University of Dayton, and Tau Technologies for developing the PANDORA sensor.

## REFERENCES

[1] Fletcher, J., "The Dynamic Optical Telescope System: Collaborative Autonomous Sensing for Space Domain Awareness," *JDR&E* **4**, 10–18 (2021).

[2] Fitzgerald, G. and et al., "Fitzgerald, G., Funke, Z., Cabello, A., Asari, V., & Fletcher, J. (2021). Toward deep-space object detection in persistent wide field of view camera arrays.," Proceedings of the Advanced Maui Optical and Space Surveillance Technologies Conference (2021).

[3] Schneider, M. D. and Dawson, W. A., "Synthesis of Disparate Optical Imaging Data for Space Domain Awareness," (Sept. 2016).

[4] Fletcher, J., McQuaid, I., and Thomas, P., "Feature-Based Satellite Detection using Convolutional Neural Networks," 11 (2019).

[5] Kelecy, T., Law, B., Sydney, P., Liang, D., Africano, J., and Paul, K., "Real-time Space Object Capture and Handoff Using Wide Field of View Telescope Development at AMOS," in [*57th International Astronautical Congress*], American Institute of Aeronautics and Astronautics (2012).

[6] Varela, L., *Streak Detection in Wide Field of View Images Using Deep Learning and Data Augmentation*, PhD thesis, New Mexico State University (2020).

[7] Grøtte, M., Virani, S., Holzinger, M., Register, A., Perez, C., Tapia, J., and Tapia Farias, J., "All-Sky Image Fusion for a Synoptic Survey Telescope in Arctic and Antarctic Domains," (Jan. 2016).

[8] Parker, L. P., Sechrest, Y. H., Vestrand, W. T., Wozniak, P., and Palmer, D., "A heterogeneous telescope array optimized for low surface-brightness imaging," in [*Ground-based and Airborne Instrumentation for Astronomy VIII*], International Society for Optics and Photonics (Dec. 2020).

[9] Zhang, C., "Robust estimation and image combining," *Astronomical Data Analysis Software and Systems* **77**(IV), 514 (1995).

[10] Ivezic, Z., Tyson, J. A., Axelrod, A., Burke, D., Claver, C. F., Kahn, S. M., Lupton, R. H., Monet, D. G., Pinto, P. A., Strauss, M. A., Stubbs, C. W., Cook, K. H., Jones, L., Saha, A., Smith, C., and LSST Collaboration, "LSST Survey Strategy," **211**, 137.02 (Dec. 2007). Conference Name: American Astronomical Society Meeting Abstracts ADS Bibcode: 2007AAS...21113702I.

[11] Jurić, Mario, e. a., "The LSST Data Management System," *arXiv preprint* **arXiv:1512.07914** (Dec. 2015).

[12] Blasch, E., Seetharaman, G., Suddarth, S., Palaniappan, K., Chen, G., Ling, H., and Basharat, A., "Summary of methods in Wide-Area Motion Imagery (WAMI)," in [*Geospatial InfoFusion and Video Analytics IV; and Motion Imagery for ISR and Situational Awareness II*], **9089**, International Society for Optics and Photonics (June 2014).

[13] Prokaj, J. and Medioni, G., "Persistent Tracking for Wide Area Aerial Surveillance," 1186–1193 (2014).
[14] Basharat, A., Turek, M., Xu, Y., Atkins, C., Stoup, D., Fieldhouse, K., Tunison, P., and Hoogs, A., "Real-time multi-target tracking at 210 megapixels/second in Wide Area Motion Imagery," in [*IEEE Winter Conference on Applications of Computer Vision*], 839–846 (Mar. 2014). ISSN: 1550-5790.
[15] Sommer, L. W., Teutsch, M., Schuchert, T., and Beyerer, J., "A survey on moving object detection for wide area motion imagery," in [*2016 IEEE Winter Conference on Applications of Computer Vision (WACV)*], 1–9 (Mar. 2016).
[16] Aspiras, T. H., Asari, V. K., and Vasquez, J., "Gaussian ringlet intensity distribution (GRID) features for rotation-invariant object detection in wide area motion imagery," in [*2014 IEEE International Conference on Image Processing (ICIP)*], 2309–2313 (Oct. 2014). ISSN: 2381-8549.
[17] Mathew, A. and Asari, V. K., "Local region statistical distance measure for tracking in Wide Area Motion Imagery," in [*2012 IEEE International Conference on Systems, Man, and Cybernetics (SMC)*], 248–253 (Oct. 2012). ISSN: 1062-922X.
[18] Ren, S., He, K., Girshick, R., and Sun, J., "Faster R-CNN: Towards Real-Time Object Detection with Region Proposal Networks," in [*Advances in Neural Information Processing Systems*], **28**, Curran Associates, Inc. (2015).
[19] He, K., Zhang, X., Ren, S., and Sun, J., "Deep Residual Learning for Image Recognition," 770–778 (2016).
[20] Redmon, J. and Farhadi, A., "YOLO9000: Better, Faster, Stronger," 7263–7271 (2017).
[21] Lin, T.-Y., Maire, M., Belongie, S., Hays, J., Perona, P., Ramanan, D., Dollár, P., and Zitnick, C. L., "Microsoft COCO: Common Objects in Context," in [*Computer Vision – ECCV 2014*], Fleet, D., Pajdla, T., Schiele, B., and Tuytelaars, T., eds., *Lecture Notes in Computer Science*, 740–755, Springer International Publishing, Cham (2014).
[22] LaLonde, R., Zhang, D., and Shah, M., "ClusterNet: Detecting Small Objects in Large Scenes by Exploiting Spatio-Temporal Information," 4003–4012 (2018).
[23] Uzkent, B., Yeh, C., and Ermon, S., "Efficient Object Detection in Large Images Using Deep Reinforcement Learning," 1824–1833 (2020).
[24] Zhou, Y. and Maskell, S., "Detecting and Tracking Small Moving Objects in Wide Area Motion Imagery (WAMI) Using Convolutional Neural Networks (CNNs)," in [*2019 22th International Conference on Information Fusion (FUSION)*], 1–8 (July 2019).
[25] Sommer, L. W., Schuchert, T., and Beyerer, J., "Fast Deep Vehicle Detection in Aerial Images," in [*2017 IEEE Winter Conference on Applications of Computer Vision (WACV)*], 311–319 (Mar. 2017).